# OPTICAL CONSTANTS OF $ZnS_xSe_{1-x}$ THIN FILMS CALCULATED FROM TRANSMISSION SPECTRA

**M. Popa[1], I. Tiginyanu[2], and V. Ursaki[2]**

[1] *"Alecu Russo" State University of Balti, Balti, Republic of Moldova*
[2] *Gitsu Institute of Electronic Engineering and Nanotechnologies, Academy of Sciences of Moldova, Chisinau, Republic of Moldova*
*ursaki@yahoo.com*

(Received March 7, 2017)

## Abstract

We report the results of calculations of some optical parameters of $ZnS_xSe_{1-x}$ thin films based on measured transmission spectra by using the Swanepoel's method, the Wemple–DiDomenico single-oscillator model, and the Sellmeier single-oscillator model. The following optical constants have been determined: refractive index $n(\lambda)$,extinction coefficient $k(\lambda)$, the $E_0$ parameter, dispersion parameter $E_d$, oscillator strength $S_0$, real $\varepsilon_1(\lambda)$ and imaginary $\varepsilon_2(\lambda)$ parts of the dielectric constant, high-frequency dielectric constant $\varepsilon_\infty$, and ratio $N/m^*$. The obtained data are in good agreement with the data for bulk ZnSe and ZnS crystals.

## 1. Introduction

II–VI compound semiconductors, especially zinc selenide (ZnSe) and zinc sulfide (ZnS), are of particular interest for researchers due to their properties relevant for the development of electronic and optoelectronic devices. These semiconductor compounds exhibit a number of important characteristics, such as good chemical and thermal stability, high optical transmission coefficient (75–95%) in the visible range, large bandgap [$E_g$ (ZnSe) = 2.67 eV and $E_g$ (ZnS) = 3.50 eV], high electrical conductivity, etc. Moreover, zinc is abundant in nature; therefore, it is a low-cost material. By combining the ZnSe and ZnS powders in certain ratios, one can obtain $ZnS_xSe_{1-x}$ ($0 < x < 1$) solid solutions; their properties can be varied in a wide range by changing their composition. $ZnS_xSe_{1-x}$ materials combine the excellent optical characteristics of ZnSe and the high mechanical resistance of ZnS. $ZnS_xSe_{1-x}$ thin films were previously prepared by various methods, such as laser ablation [1], high-pressure sputtering [2], molecular beam epitaxy [3], atomic layer epitaxy [4], metalorganic atomic layer epitaxy [5], metal organic vapor phase epitaxy [6], and close-spaced evaporation [7].

Studies of the optical properties of thin semiconductor films, such as transmission, reflection, and absorption spectra, refractive index dispersion, as well as impact of thermal treatment upon these properties, provide important information about the energy band structure and the mechanisms of electromagnetic radiation interaction with the thin layer. By correlating these data with those obtained from electrical transport phenomena, one can extract specific information about the general characteristics of the studied thin films.

The goal of this paper is to present the calculated and extrapolated values of some optical parameters, as well as their dispersion, from the measured transmission spectra of $ZnS_xSe_{1-x}$ thin films. We show that some data about the structure of the studied films can be deduced from the

analysis of the lower limit of the transmission spectrum. Particularly, one can conclude that the semiconductor compound has no deviation from stoichiometry and the defect concentration is low, if the transmission spectrum exhibits a sharp edge at long wavelength at room temperature.

## 2. Experimental

Thin $ZnS_xSe_{1-x}$ ($x$ = 0; 0.2, 0.4, 0.5, 0.6, 0.8, 1.0) films with thickness between 0. 2 and 1.0 mm were prepared on corning glass substrates by thermal evaporation under vacuum using a VUP-5 quasi-closed volume instrument. The temperature of the source material $T_{ev}$ was measured by a Pt/PtRh thermocouple and varied in a range of 700–1500 K. The substrate temperature was measured with a Fe–CuNi (constantan) thermocouple (or with a NiCr/NiAl thermocouple) and was maintained at 300 K. XRD analysis revealed a cubic zinc blende structure of the prepared films with a preferential orientation of the (111) planes parallel to the substrate. Atomic force microscopy (AFM), scanning electron microscopy (SEM), and energy-dispersive X-Ray (EDX) analysis showed that the films are homogeneous, continuous, and stoichiometric. Three different methods were used to measure the film thickness:

a) the *interferometric method* [8, 9] based on the interference of two monochromatic radiation beams reflected from the substrate and the film surfaces;
b) the *optical method* [10–16] based on refractive index dispersion as described below; and
c) *cross-sectional SEM images*.

The results obtained by these methods are very close to each other.

The transmission spectra of $ZnS_xSe_{1-x}$ films were measured in a spectral range of 330–1750 nm by means of a HITACHI U-3400 spectrometer.

## 3. Experimental Results

### *3.1. Transmission spectra of $ZnS_xSe_{1-x}$ thin films*

The transmission spectra of $ZnS_xSe_{1-x}$ samples were analyzed as a function of layer thickness and the $x$ parameter. The thickness of thin layers is an important parameter in studying the optical and photoelectrical properties, since layers with definite thicknesses can be obtained.

Optical transmission spectra are shown in Fig. 1 for six $ZnS_xSe_{1-x}$ thin layers with varying thickness. The transmittance of the sample with a thickness of $d$ = 0.15 μm (Fig. 1*a*) sharply increases up to a maximum value and then monotonously deceases in a spectral range of 600–900 nm. At wavelengths longer than 900 nm, transmittance slightly depends on wavelength. Two, three, four, and five transmission maxima are revealed in the transmission spectrum of the sample with $d$= 0.25 μm (Fig. 1b), $d$ = 0.45 μm (Fig. 1c), $d$ = 0.60 μm (Fig. 1d), and $d$ = 0.77 μm (Fig. 1e), respectively. The transmission spectra of samples thicker than 0.80 μm (Fig. 1f) consist of a series of maxima and minima; the difference between the maximum and minimum transmission decreases with increasing the $ZnS_{0.5}Se_{0.5}$ layer thicknesses. A similar behavior is observed for other $ZnS_xSe_{1-x}$ layers.

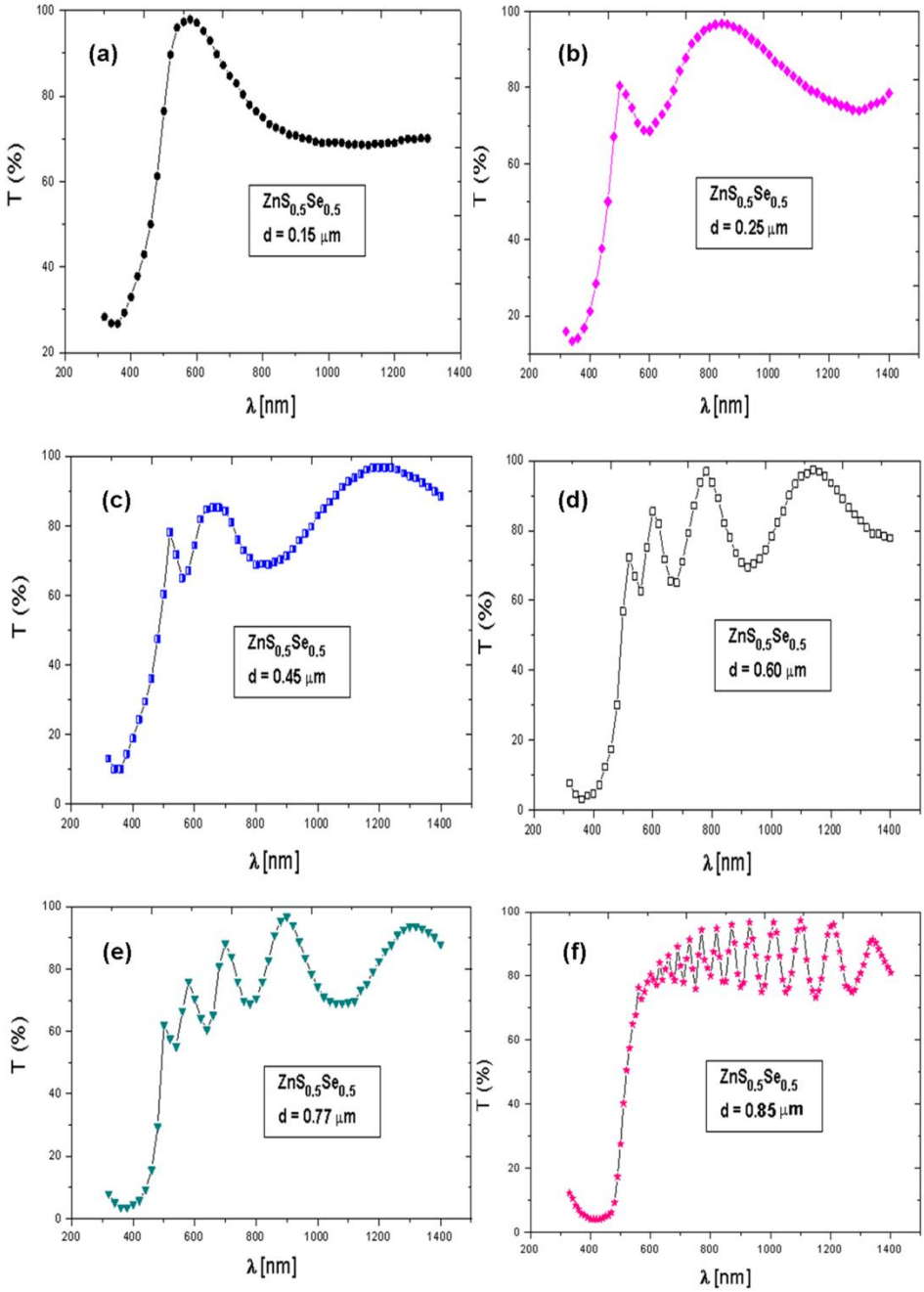


**Fig. 1**. Evolution of the transmission spectra of thin $ZnS_xSe_{1-x}$ films as a function of their thickness.

The presence of fringes (maxima and minima) in the transmission spectra due to interference of light beams through multiple reflections at the air-layer interfaces suggests that the layers thickness is uniform and that the surfaces are parallel to each other. This observation was confirmed by AFM analysis [16], which also revealed a low surface roughness. A high roughness or thickness non-uniformity would compromise the interference and would lead to the disappearance of maxima and minima in the transmission spectra [10–13]. The dependence of spectra on the *x* values was also studied (Fig. 2). A shift of the fundamantal absorption edge to lower wavelengths from 420 nm to 300 nm with increasing the *x* value is observed.

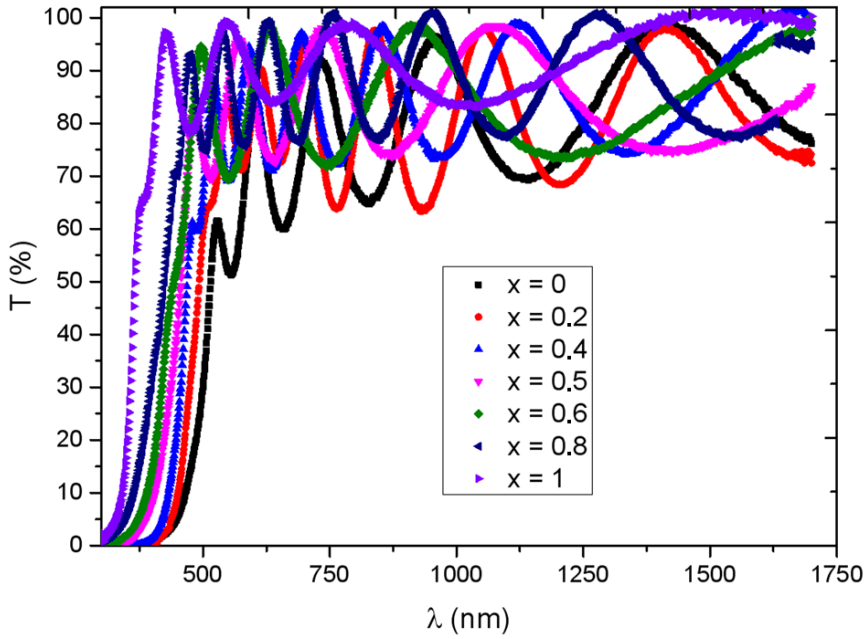


**Fig. 2**. Evolution of the transmission spectra of thin $ZnS_xSe_{1-x}$ films as a function of the *x* value.

### *3.2. Determination of the refractive index of $ZnS_xSe_{1-x}$ thin films*

The optical properties of thin films significantly depend on the preparation technology. Refractive index *n* and extinction coefficient *k* (absorption index) are two of the most important optical constants. The refractive index of $ZnS_xSe_{1-x}$ films was determined from the optical transmission spectra by using the envelope method proposed by Swanepoel [10–13]. Let us consider a thin homogeneous layer with a uniform thickness *d* and complex refractive index $\tilde{n} = n - ik$, where *n* is the refractive index and *k* is the extinction coefficient. The layer is deposited on a transparent smooth substrate with refractive index $n_s$ and a much larger thickness than that of the layer, the absorption coefficient of the substrate being negligible. This system being placed in air with refractive index $n_0 = 1$ is illustrated in Fig. 3.

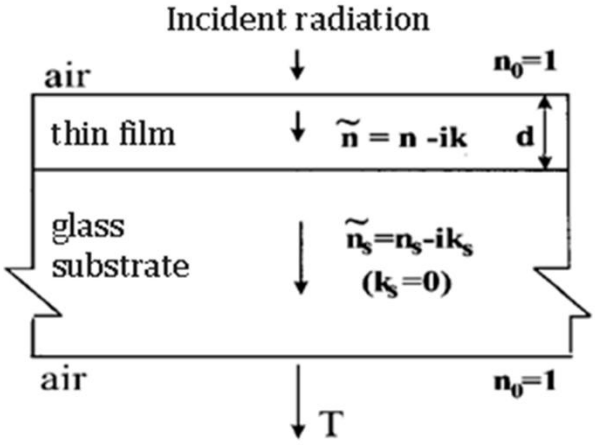


**Fig. 3**. Schematic film–substrate system used in the Swanepoel method.

The transmission spectra exhibits a series of maxima and minima (Fig. 4), i.e., one should take into account the interference due to multiple reflections inside the layer for a thorough analysis of these spectra. Basically, the Swanepoel method consists in the determination of minima and maxima envelopes in the transmission spectra (Fig. 4). Thereby, for a certain wavelength, one can found a pair of $T_M$ and $T_m$ values with expressions deduced below.

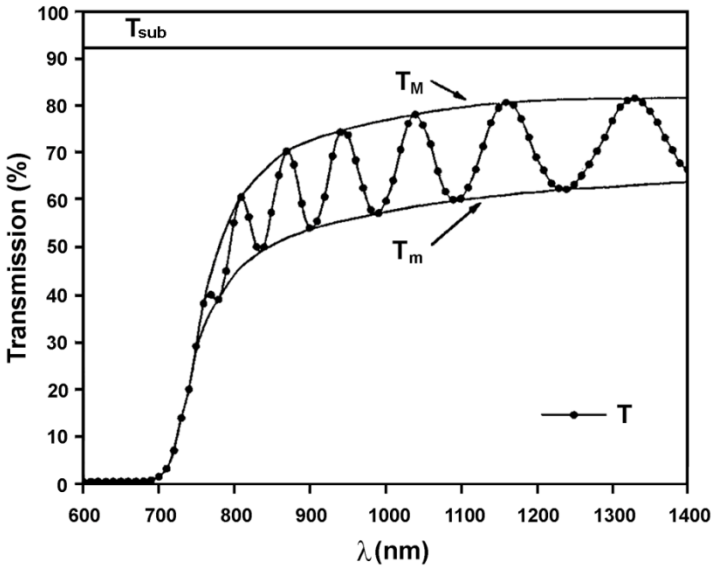


**Fig. 4**. Interference maxima and minima in the transmission spectrum.

For the system illustrated in Fig. 3, the optical transmission at a normal incidence can be expressed as follows [1, 10–13]:

$$T = \frac{Ax}{B - Cx\cos\phi + Dx^2}, \tag{1}$$

where

$$\left\{\begin{array}{l} A = 16n^2 n_s \\ B = (n+1)^3 (n + n_s^2) \\ C = 2(n^2 - 1)(n^2 - n_s^2 \\ D = (n-1)^3 (n - n_s^2) \\ \psi = \dfrac{4\pi nd}{\lambda} \\ x = \exp(-\alpha d) \end{array}\right\} \tag{2}$$

and $d$ is the layer thickness.

The values of transmission at the interference fringes ($T_M$ and $T_m$) are obtained from the interference condition $\cos\psi = +1$ for the maximum and $\cos\psi = -1$ for the minimum, or from the following condition [1, 10–16]:

$$2nd = m\lambda, \tag{3}$$

where $m$ is an integer number for the maxima and a half-integer for the minima of interference.

Under these conditions, the maxima and minima of interference are situated in two curves referred to as envelopes; $T_M$ and $T_m$ (Fig. 2) are calculated from the following relationships [1, 10–13]:

$$T_M = \frac{Ax}{B - Cx + Dx^2} \tag{4}$$

and

$$T_m = \frac{Ax}{B + Cx + Dx^2}. \tag{5}$$

It should be noted that these relationships are valid only in the spectral range where the absorption is weak or medium, so that the coefficient of extinction $k$ can be neglected. In this case, from Eqs. (4) and (5), one can deduce

$$\frac{1}{T_M} - \frac{1}{T_m} = \frac{2C}{A} \tag{6}$$

By calculating $A$ and $C$ from (2), we obtain [1, 10–13]

$$n = \sqrt{N + \sqrt{(N^2 - n_s^2}}\ , \tag{7}$$

where

$$N = 2n_s \frac{T_M - T_m}{T_M T_m} + \frac{n_s^2 + 1}{2}. \tag{8}$$

The refractive index calculated from (7) can be considered as a first approximation. If the layer thickness is known, then the interference order $m$ can be determined by using Eq. (3). The obtained values will be approximated as integer or half-integer, because their transmission spectrum represents a maximum or a minimum at the respective wavelength. By using these values and Eq. (3), the new values of the refractive index can be calculated.

The thickness of the thin film can also be calculated from the transmission spectrum, if the refractive indices $n_1$ and $n_2$ are known for the two adjacent maxima (or minima) with wavelength $\lambda_1$ and $\lambda_2$, by using the following relationship [10–16]:

$$d = \frac{\lambda_1 \lambda_2}{2(\lambda_1 n_2 - \lambda_2 n_1)}. \tag{9}$$

Formula (9) is very sensitive to the errors of $n$ and cannot provide a high precision.
The steps for calculating the refractive index of thin $ZnS_xSe_{1-x}$ films are as follows:

a) calculation of the refractive index of the substrate $n_s$ from transmission spectrum $T_{sub} = f(\lambda)$ by means of the following relationship [10–16]:

$$n_s = \frac{1}{T_{sub}} - \sqrt{\left(\frac{1}{T_{sub}^2} - 1\right)} \tag{10}$$

b) drawing the envelopes of interference minima and maxima in the transmission spectrum of a thin film $T = f(\lambda)$ and determination of the $T_M$ and $T_m$ pairs for each wavelength;
c) calculation of the $N$ coefficient by using Eq. (8); and
d) calculation of $n$ values by using Eq. (7).

The glass substrates used for the deposition of thin $ZnS_xSe_{1-x}$ films exhibit an almost constant transmission in the studied spectral range, it being varied by only 0.5% from 92.0% at $\lambda$ = 600 nm to 92.5% at $\lambda$ = 1400 nm. Therefore, a value of 92.3% was used for the optical transmission in all calculations, which represents a mean value for the considered spectral range

(Fig. 4).

The dispersion of the refractive index for seven thin $ZnS_xSe_{1-x}$ films is shown in Fig. 5. One can see that the refractive index decreases with an increase in both the radiation wavelength and the value of $x$ (i.e., an increase in the sulphur content and a decrease in the selenium content) for each of the studied samples. For instance, the refractive index measured at $\lambda$ = 616 nm decreases from $n$ = 2.77 for $x$ = 0 to $n$ = 2.27 for $x$ = 1, while for $\lambda$ = 1726 nm the refractive index decreases from $n$ = 2.06 for $x$ = 0 to $n$ = 1.95 for $x$ = 1. This decrease correlates with the increase in the transmission coefficient and the decrease in the absorption coefficient. On the other hand, this evolution is probably due to a decrease in the crystallite size and an increase in the layer compactness [16].

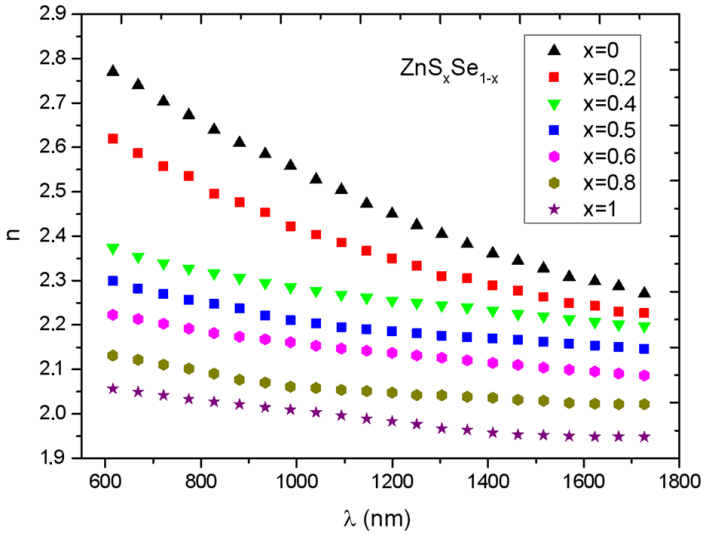


**Fig. 5**. Dispersion of the refractive index of $ZnS_xSe_{1-x}$ films.

Each of the $n(\lambda)$ dependences were extrapolated by quadratic dispersion relations according to the modes shown in Fig. 6. The refractive index dispersion relations for $ZnS_xSe_{1-x}$ films are summarized in Table 1.

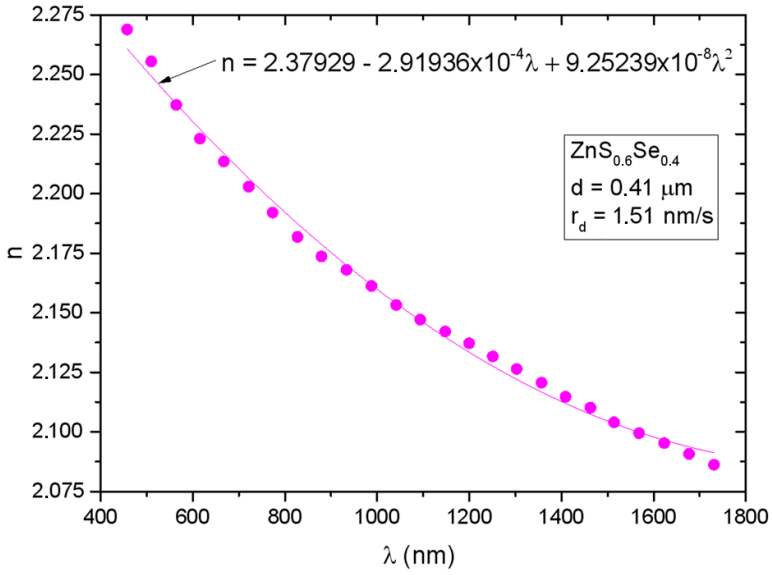


**Fig. 6**. Dispersion of the refractive index of a $ZnS_{0.6}Se_{0.4}$ film.

**Table 1**. Dispersion relationship $n = f(\lambda)$ for $ZnS_xSe_{1-x}$ thin films

| Sample number | *X* value | $n = f(\lambda)$ |
|---|---|---|
| 1 | 0 | $3.26732 - 0.00102\lambda + 2.69969 \times 10^{-7}\lambda^2$ |
| 2 | 0.2 | $3.05717 - 8.44061 \times 10^{-4}\lambda + 2.10684 \times 10^{-7}\lambda^2$ |
| 3 | 0.4 | $2.58808 - 5.80716 \times 10^{-4}\lambda + 1.43421 \times 10^{-7}\lambda^2$ |
| 4 | 0.5 | $2.51703 - 4.31306 \times 10^{-4}\lambda + 1.28291 \times 10^{-7}\lambda^2$ |
| 5 | 0.6 | $2.37929 - 2.91936 \times 10^{-4}\lambda + 9.25239 \times 10^{-8}\lambda^2$ |
| 6 | 0.8 | $2.27222 - 2.88166 \times 10^{-4}\lambda + 8.33986 \times 10^{-8}\lambda^2$ |
| 7 | 1 | $2.18828 - 2.27322 \times 10^{-4}\lambda + 4.97754 \times 10^{-8}\lambda^2$ |

Ilenikhena [17] reported a variation in the refractive index from 1.14 to 2.59 at photon energies of 1.46 eV (λ = 850 nm) and 4.14 eV (λ = 300 nm) for ZnS thin films deposited by chemical reactions. It was recommended that the materials with a low value of the refractive index can be used in antireflection coatings. This kind of films with refractive index lower than 1.9 can be used to decrease the reflection coefficient from 0.36 to 0.04 in photovoltaic devices and increase the transmission up to 0.91–0.96 [18, 19]. Connolly [20] reported a dispersion of the refractive index from 2.598 (λ = 621 nm) to 2.451 (λ = 1724 nm) with a dispersion rate of $dn/d\lambda = -0.8676\ \mu m^{-1}$, while Marple [21] measured the dispersion of refractive index $n(\lambda)$ between 2.586 (λ = 621 nm) and 2.444 (λ = 1732 nm) with a dispersion rate of $dn/d\lambda = -0.8830\ \mu m^{-1}$. Similar dispersions of the refractive index were reported for $ZnS_xSe_{1-x}$ thin films by Ambrico [1] and Venkata Subbaiah [7].

### *3.3. The Wemple–DiDomenico single-oscillator model*

According to the single-oscillator model proposed by Wemple and DiDomenico [1, 12–16, 22, 23], the refractive index dispersion in the transparency spectral region (for photon energies lower than the bandgap) can be described by the following relationship:

$$n^2 - 1 = \frac{E_0 E_d}{E_o^2 - (h\nu)^2} \tag{11}$$

where $E_0$ is a parameter whose value is approximately equal to double the value of the bandgap ($E_0 \cong 2E_g^{opt}$), $h\nu$ is the photon energy, and $E_d$ is the dispersion parameter.

Relationship (11) can be transformed as follows:

$$\frac{1}{n^2 - 1} = \frac{E_0}{E_d} - \frac{(h\nu)^2}{E_0 E_d} \tag{12}.$$

A straight line is obtained by plotting the graph $(n^2 - 1)^{-1} = f(h\nu)^2$; from the slope of this line, the following term can de determined:

$$E_0 E_d = \frac{(h\nu)_2^2 - (h\nu)_1^2}{\left(\frac{1}{n^2 - 1}\right)_2 - \left(\frac{1}{n^2 - 1}\right)_1} \tag{13}$$

The $E_0^2 = (h\nu)^2$ value is obtained by extrapolating the graph for the case of $1/(n^2 - 1) \to 0$.

By using these data, one can calculate the $E_d$ value.

Figure 7 presents the $(n^2 - 1)^{-1} = f(h\nu)^2$ dependences for $ZnS_xSe_{1-x}$ thin films on glass substrates. The $E_d$ and $E_0$ values were determined from the slope of the linear dependence, which are listed in Table 2. The $E_0/E_g$ values lie in a range of 1.98–2.02. Dispersion energy $E_d$ is a measure of the mean strength of optical interband transitions. Wemple [22] found that $E_d$ does not depend on the bandgap or on the electron concentration; instead, it obey a simple empirical relation:

$$E_d = \beta N_c Z_a N_e \tag{14}$$

where $N_c$ is the coordination number of the nearest cation to the anion, $Z_a$ is the chemical valence of the anion, and $N_e$ is the effective number of valence electrons on the anions. Coefficient β is a second rank parameter; it represents an indicative of the chemical bond in the crystal structure. The β value can be less than unity; it was estimated to be equal to $\beta_i = 0.26 \pm 0.04$ for the ionic bond in halides and oxides, while for covalent bonds in zincblende, scheelite, and diamond-type structures it is $\beta_c = 0.37 \pm 0.05$. The bonds are highly covalent in pure crystalline ZnS and ZnSe compounds, and the calculated $\beta_c$ proved to be 0.41 for ZnS and 0.42 for ZnSe [22].

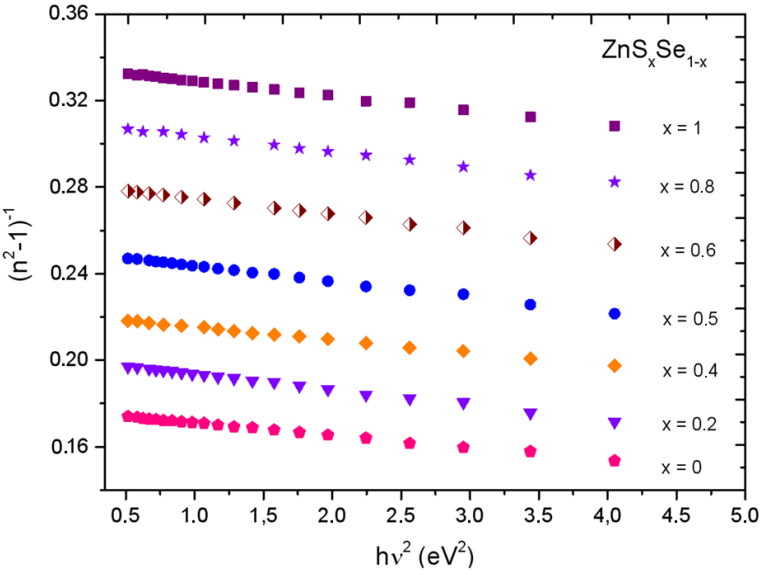


**Fig. 7**. $(n^2 - 1)^{-1} = f(h\nu)^2$ graphs for $ZnS_xSe_{1-x}$ films.

**Table 2.** Dispersion parameters deduced from the Wemple–DiDomenico single-oscillator model

| **Sample number** | **Composition** | ***d*, µm** | **$r_d$, nm/s** | **$T_{sub}$, *K*** | **$E_0$, eV** | **$E_d$, eV** | **$E_0/E_g$** |
|---|---|---|---|---|---|---|---|
| 1 | ZnSe | 0.55 | 1.73 | 300 | 5.28 | 26.86 | 1.98 |
| 2 | $ZnS_{0.2}Se_{0.8}$ | 0.71 | 1.82 | 300 | 5.57 | 25.46 | 2.00 |
| 3 | $ZnS_{0.4}Se_{0.6}$ | 0.78 | 1.86 | 300 | 5.78 | 24.39 | 2.02 |
| 4 | $ZnS_{0.5}Se_{0.5}$ | 0.52 | 1.73 | 300 | 6.12 | 23.66 | 1.99 |
| 5 | $ZnS_{0.6}Se_{0.4}$ | 0.41 | 1.51 | 300 | 6.32 | 22.81 | 2.00 |
| 6 | $ZnS_{0.8}Se_{0.2}$ | 0.22 | 1.23 | 300 | 6.70 | 21.56 | 2.01 |
| 7 | ZnS | 0.41 | 1.52 | 300 | 7.07 | 20.88 | 2.02 |

### 3.4. The Sellmeier single-oscillator model

Refractive index dispersion can also be expressed according to the Sellmeier dispersion relation for most of materials [24]:

$$n^2 - 1 = \frac{S_0 \lambda_0^2}{\lambda_0^2 - \lambda^2}, \tag{15}$$

where $S_0$ is the oscillator strength with wavelength $\lambda_0$ ($E_0 = hc/\lambda_0$).

Similarly to the previous case, Eq. (15) can be transformed to the form

$$\frac{1}{n^2 - 1} = \frac{1}{S_0 \lambda_0^2} - \frac{1}{S_0 \lambda^2} \tag{16}$$

and, by plotting the $(n^2 - 1)^{-1} = f\,(1/\lambda^2)$ graph, a straight line is obtained. The following term is determined from the slope of this line:

$$S_0 = \frac{\left(\frac{1}{\lambda_2^2} - \frac{1}{\lambda_1^2}\right)}{\left(\frac{1}{n^2 - 1}\right)_2 - \left(\frac{1}{n^2 - 1}\right)_1} \tag{17}$$

The $1/\lambda_0^2 = 1/\lambda^2$ value is obtained by extrapolating the graph for the case of $1/(n^2 - 1) \to 0$, from which it follows that $\lambda_0 = \lambda$.

Figure 8 presents the $(n^2 - 1)^{-1} = f\,(1/\lambda^2)$ dependences for thin $ZnS_xSe_{1-x}$ films deposited on glass substrates. The $\lambda_0$ and $S_0$ values were obtained from the slope of the linear dependence, which are shown in Table 3.

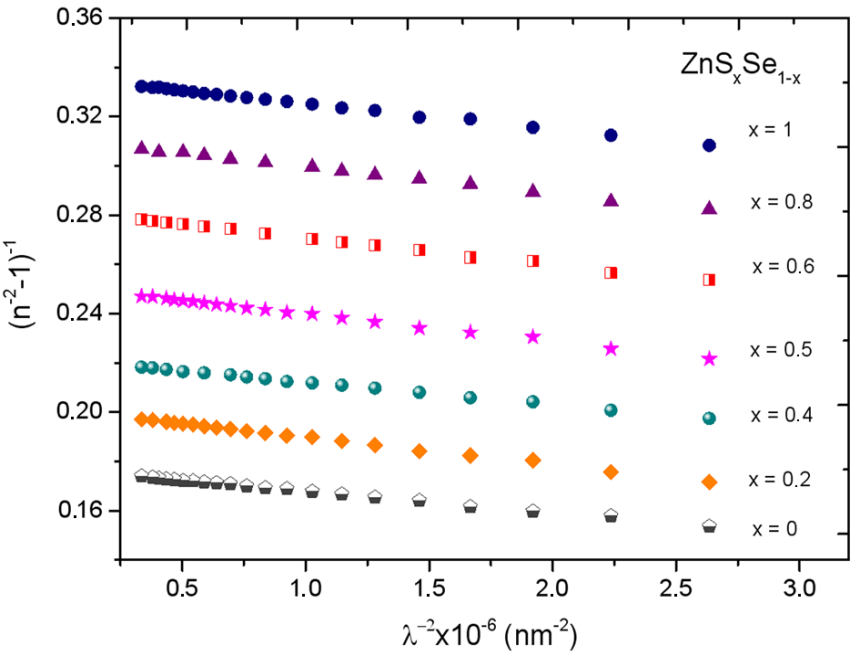


**Fig. 8**. Sellmeier single-oscillator model for $ZnS_xSe_{1-x}$ films.

**Table 3.** Dispersion parameters determined from the Sellmeier single-oscillator model

| **Sample number** | **Composition** | ***d*, μm** | **$r_d$, nm/s** | **$\lambda_0$, nm** | $S_0 \cdot 10^{14}$, $m^{-2}$ |
|---|---|---|---|---|---|
| 1 | ZnSe | 0.55 | 1.73 | 224 | 26.86 |
| 2 | $ZnS_{0.2}Se_{0.8}$ | 0.71 | 1.82 | 217 | 25.46 |
| 3 | $ZnS_{0.4}Se_{0.6}$ | 0.78 | 1.86 | 209 | 24.39 |
| 4 | $ZnS_{0.5}Se_{0.5}$ | 0.52 | 1.73 | 200 | 23.66 |
| 5 | $ZnS_{0.6}Se_{0.4}$ | 0.41 | 1.51 | 192 | 22.81 |
| 6 | $ZnS_{0.8}Se_{0.2}$ | 0.22 | 1.23 | 186 | 21.56 |
| 7 | ZnS | 0.41 | 1.52 | 175 | 20.88 |

### *3.5. Determination of the extinction coefficient of $ZnS_xSe_{1-x}$ thin films*

The imaginary part of refractive index $\tilde{n}$ represents extinction coefficient $k$, which is a measure of the light amount lost due to the scattering and absorption on the unity of penetrating distance into the medium.

The extinction coefficient of thin films can be calculated from the following relation [1, 7, 10, 13, 14]:

$$k = \frac{\alpha\lambda}{4\pi} \tag{18}$$

where $\alpha$ is the absorption coefficient, which, in the region of weak and medium absorption, is determined by the following relationship [10, 13, 14]:

$$x = \exp(-\alpha d) \Rightarrow \alpha = \frac{1}{d}\ln\frac{1}{x} \tag{19}$$

Absorptance $x$ can be determined by one of the several methods proposed by Swanepoel:

(i) If the data of maximum transmission $T_M$ are used, then absorbance is determined according to the following relationship [10, 13, 14]:

$$x = \frac{E_M - [E_M^2 - (n^2-1)^3(n^2-n_S^4)]^{1/2}}{(n-1)^3(n-n_S^2)}, \tag{20}$$

where

$$E_M = \frac{8n^2 n_S}{T_M} + (n^2-1)(n^2-n_S^2). \tag{21}$$

(ii) By using the data of minimum transmission $T_m$, one can determine the absorbance from the following relationship [10]:

$$x = \frac{E_m - [E_m^2 - (n^2-1)^3(n^2-n_S^4)]^{1/2}}{(n-1)^3(n-n_S^2)}, \tag{22}$$

where

$$E_m = \frac{8n^2 n_s}{T_m} - (n^2-1)(n^2-n_s^2). \tag{23}$$

(iii) By using both the data of maximum transmission $T_M$ and minimum transmission $T_m$, the absorptance can be determined according to the following relationship [1, 10]:

$$x = \frac{F - [F^2 - (n^2 - 1)^3 (n^2 - n_S^4)]^{1/2}}{(n-1)^3 (n - n_S^2)}, \tag{24}$$

where

$$F = \frac{8n^2 n_S}{T_i} \tag{25}$$

and

$$T_i = \frac{2T_M T_m}{T_M + T_m}. \tag{26}$$

We performed calculations for our samples according to all the above described models; the evolution of extinction coefficient $k$ proved to be similar. Figure 9 shows the $k(\lambda)$ graphs for seven $ZnS_xSe_{1-x}$ thin films calculated according to Eqs. (24)–(26). One can observe that extinction coefficient $k$ is more than one hundred times smaller that refractive index $n$ and increases insignificantly with increasing wavelength. The low values of the extinction coefficient can be associated with the low values of the absorption coefficient in the respective wavelength range.

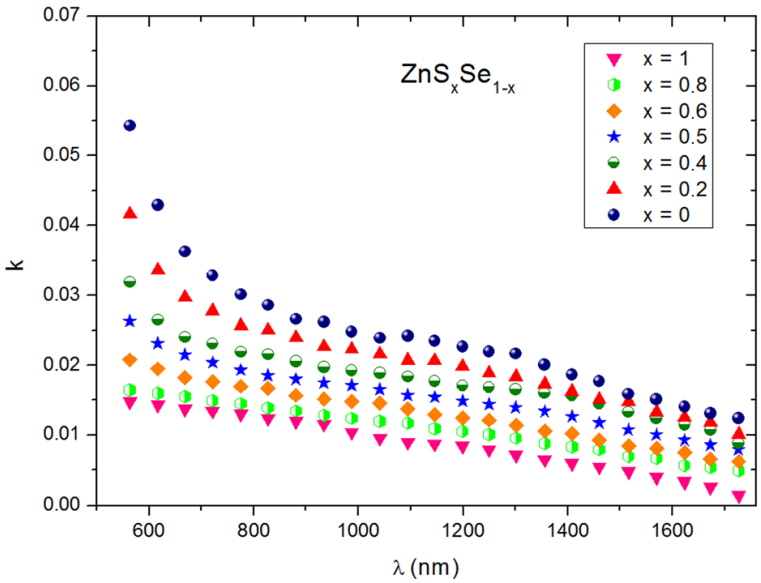


**Fig. 9**. Dependence of the extinction coefficient on the wavelength for $ZnS_xSe_{1-x}$ thin films.

Ilenikhene [17] reported variations in the extinction coefficient between $0.867 \times 10^2$ and $1.127 \times 10^2$ for thin ZnS films deposited by chemical reactions.

### *3.6. Determination of the dielectric constant of $ZnS_xSe_{1-x}$ thin films*

The dielectric constant of a solid consists of real $\varepsilon_1$ and imaginary $\varepsilon_2$ parts [15]:

$$\hat{\varepsilon} = \varepsilon_r + i\varepsilon_I = \hat{n}^2 = (n \pm ik)^2 = (n^2 - k^2) + i2nk, \tag{27}$$

which in turn depend on refractive index $n$ and extinction coefficient $k$ [15]:

$$\varepsilon_r = n^2 - k^2, \; \varepsilon_I = 2nk. \tag{28}$$

The dependences of the real and imaginary parts of the dielectric constant on the wavelength $\varepsilon_r(\lambda)$ and $\varepsilon_I(\lambda)$ are shown in Figs. 10 and 11. One can see that the real part decreases with an increase in both wavelength $\lambda$ and the *x* value (an increase in the content of sulfur S and a decrease in the content of selenium Se) (Fig. 10). The value of the imaginary part is more than one hundred times lower than that of the real part; it increases with an increase in both wavelength $\lambda$ and the *x* value (Fig. 11).

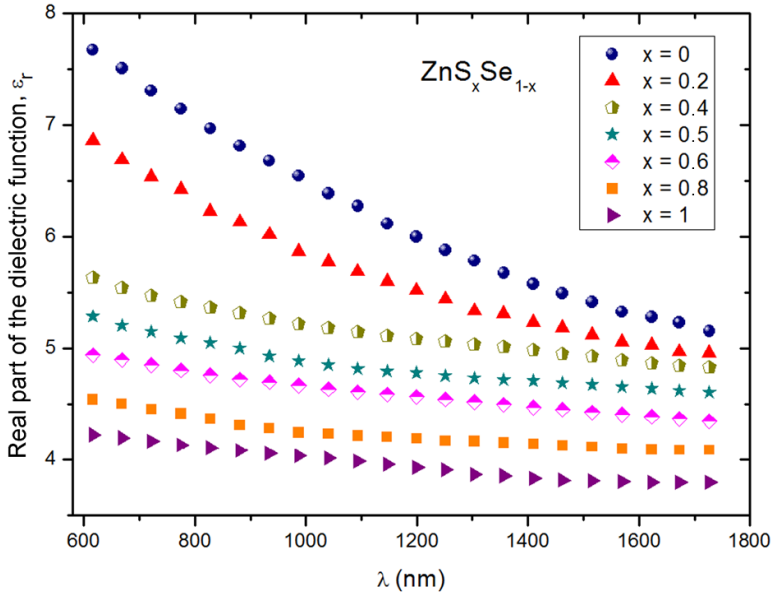


**Fig. 10**. Dependence of the real part of the dielectric constant on the wavelength for $ZnS_xSe_{1-x}$ thin films.

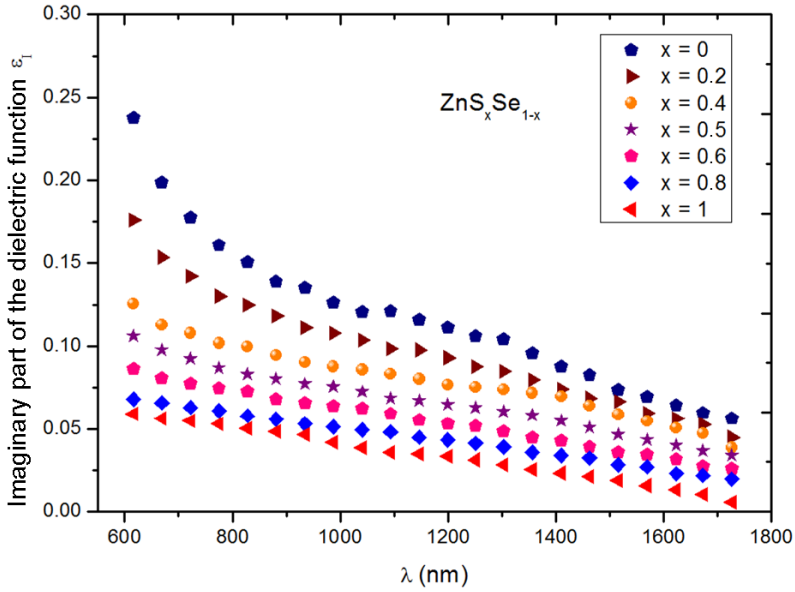


**Fig. 11**. Dependence of the imaginary part of the dielectric constant on the wavelength for $ZnS_xSe_{1-x}$ thin films.

On the other hand, the dependence of the real part of the dielectric constant of a solid on the wavelength is given by the following relationship:

$$\varepsilon_r = \varepsilon_\infty - \left(\frac{e^2}{4\pi^2 c^2 \varepsilon_0}\right)\left(\frac{N}{m^*}\right)\lambda^2, \tag{29}$$

where $N/m^*$ is the electron concentration to effective mass ratio, $c$ is the speed of light in the vacuum, $\varepsilon_0$ is the permittivity of the vacuum, and $e$ is the electron charge.

The graphs $\varepsilon_r = f(\lambda^2)$ shown in Fig. 12 contain a linear segment. By extrapolating these graphs to $\lambda^2 = 0$, one can obtain the high frequency dielectric constant $\varepsilon_\infty = \varepsilon_r (\lambda^2 = 0)$, and the value of the $N/m^*$ ratio is determined from the slope of these graphs for $ZnS_xSe_{1-x}$ thin films according to the relationship:

$$\frac{N}{m^*} = \left(\frac{4\pi^2 c^2 \varepsilon_0}{e^2}\right)\frac{\varepsilon_{r1} - \varepsilon_{r2}}{\lambda_2^2 - \lambda_1^2} \tag{30}$$

The $\varepsilon_\infty$ and $N/m^*$ values of $ZnS_xSe_{1-x}$ thin films are listed in Table 4.

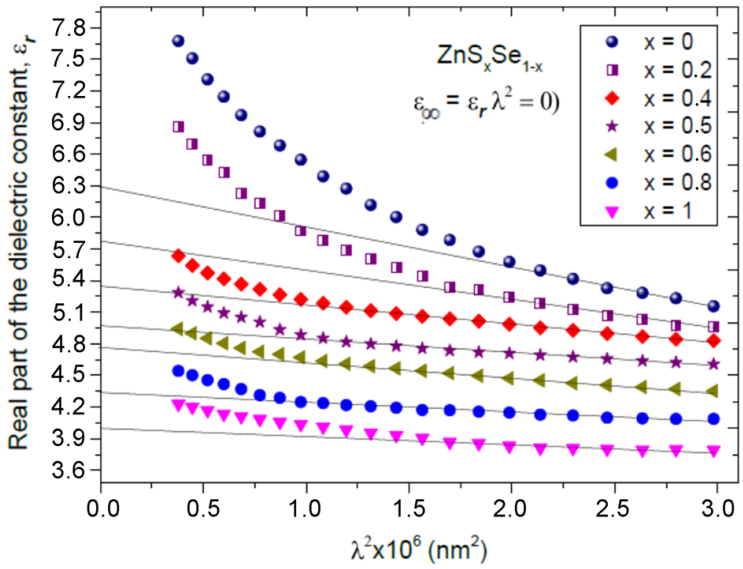


**Fig. 12**. Dependence of the dielectric constant on the wavelength for $ZnS_xSe_{1-x}$ thin films.

**Table 4.** Values of high-frequency dielectric constant and electron concentration to effective mass ratio for $ZnS_xSe_{1-x}$ thin films

| Sample number | Composition | $d$, μm | $r_d$, nm/s | $\varepsilon_\infty$ | $N/m^* \cdot 10^{47}$, cm$^{-3}$/g |
|---|---|---|---|---|---|
| 1 | ZnSe | 0.55 | 1.73 | 6.30 | 5.20 |
| 2 | $ZnS_{0.2}Se_{0.8}$ | 0.71 | 1.82 | 5.78 | 3.60 |
| 3 | $ZnS_{0.4}Se_{0.6}$ | 0.78 | 1.86 | 5.35 | 2.20 |
| 4 | $ZnS_{0.5}Se_{0.5}$ | 0.52 | 1.73 | 4.96 | 1.77 |
| 5 | $ZnS_{0.6}Se_{0.4}$ | 0.41 | 1.51 | 4.77 | 1.34 |
| 6 | $ZnS_{0.8}Se_{0.2}$ | 0.22 | 1.23 | 4.35 | 0.99 |
| 7 | ZnS | 0.41 | 1.52 | 4.00 | 0.70 |

The obtained values are consistent with those reported in the literature. Ruda [25] reported

high-frequency dielectric constant values of 6.2 for ZnSe and 4.5 for ZnS.

## 4. Conclusions

The results of this study show the possibility of depositing $ZnS_xSe_{1-x}$ thin films with a cubic zincblende structure with a strong orientation in the (111) crystallographic plane on glass substrates by means of thermal evaporation in a vacuum. The optical transmission spectra exhibit a series of maxima and minima due to the interference of light beams multiple reflected from the layer surfaces. It is found that the dispersion of refractive index $n(\lambda)$ is negative, while that of extinction coefficient $k(\lambda)$ is positive. The $E_0$ parameter determined according to the Wemple–DiDomenico single-oscillator model varies for $ZnS_xSe_{1-x}$ thin films in a range of 5.28–7.07 eV as a function of $x$ value, it being approximately equal to double the value of the bandgap, while dispersion parameter $E_d$ varies in a range of 28.86–20.88 eV. The oscillator strength value deduced according to the Sellmeier single-oscillator model varies in a range of $S_0 = 26.86 \times 10^{14}$ to $20.88 \times 10^{14}$ $m^{-2}$, with wavelength $\lambda_0$ ($E_0 = hc/\lambda_0$) varying in a range of 224–175 nm. High-frequency dielectric constant $\varepsilon_\infty$ deduced from the slope of the $\varepsilon_r(\lambda)$ dispersion lies in a range of 6.30 for ZnSe to 4.00 for ZnS, while the $N/m^*$ ratio varies in a range of $5.20 \times 10^{47}$ to $0.70 \times 10^{47}$ $cm^{-3}/g$.

## References


[1] M. Ambrico, G. Perna, D. Smaldone, C. Spezzacatena, V. Stagno, and V. Capozzi, Semicond. Sci. Technol. 13, 1446, (1998).
[2] A. Ganguly, S. Chaudhury, and A. K. Pal, J. Phys. D: Appl. Phys. 34, 506, (2001).
[3] L. S. Lai, I. K. Sou, C. W. Y. Law, K. S. Wong, Z. Yang, and G. K. L. Wong, Opt. Mater. 23, 21, (2003).
[4] C. T. Hsu, Mater. Chem. Phys. 58, 6, (1999).
[5] J. H Song, E. D Sim, K. S Baek, and S. K Chang, J. Cryst. Growth 214–2015, 460 (2000).
[6] P. Prete, N. Lovergine, S. Petroni, G. Mele, A. M Mancini, and G. Vasapollo, Mater. Chem. Phys. 66, 253, (2000).
[7] Y. P. Venkata Subbaiah, P. Prathap, K.T.R. Reddy, D. Mangalaraj, K. Kim, and Y. Junsin, J. Phys. D: Appl. Phys. 40, 3683, 40, (2007).
[8] I. Spanulescu, Fizica straturilor subţiri şi aplicaţiile acestora, Ed. Stiinţifică, Bucureşti, 1975, 320 p.
[9] K. L. Chopra, Thin film phenomena, McGraw-Hill, New York 1969, 736 p.
[10] R. Swanepoel, J. Phys. E: Sci. Instrum. 16, 1214, (1983).
[11] R. Swanepoel, J. Phys. E: Sci. Instrum. 17, 896, (1984).
[12] E. Margues, J. Ramires-Malo, P. Villares, R. Jimenes-Garay, P. J. Ewen, and A. E. Owen, J. Phys. D: Appl. Phys. 25, 535, (1992).
[13] E. Margues, J. B. Ramires-Malo, P. Villares, R. Jimenes-Garay, and R. Swanepoel, Thin Solid Films 254, 83, (1995).
[14] L. Meng, M. Andritschky, and M. P. Dos Santos, Thin Solid Films 223, 247, (1993).
[15] A. H. Clark, Optical Properties of Polycrystalline Semiconductor Films in Polycrystalline and Amorphous Thin Films and Devices, in Polycrystalline and Amorphous Thin Film and Device, Lawrence Kazmerski (Ed), Academic Press, New York, 1980, p. 135-152.

[16] M. Popa, Cercetari privind structura si morfologia suprafetei, proprietatile electrice, optice si luminiscente ale straturilor subtiri semiconductoare de ZnSe, Iasi, Ed-ra PIM, 2014, 186 p.
[17] P. A. Ilenikhena, Afr. Phys. Rev. 2, 7, (2008).
[18] C. J. Brinker, Sol. Energy Mater. 5, 159, (1981).
[19] R.B. Pettit and C.J. Brinker, Sol. Energy Mater. 14, 269, (1986).
[20] J. Connolly, B. DiBenedetto, and R. Donadio, Proc. SPIE, 181, 141, (1979).
[21] D. T. F. Marple, J. Appl. Phys. 35, 539, (1964).
[22] S. H. Wemple and M. DiDomenico, Phys. Rev. B 3, 1338, (1971).
[23] S. H. Wemple, Phys. Rev. B 7, 3767, (1973).
[24] T. Berge, Appl. Opt. 23, 4477, (1984).
[25] H. E. Ruda, Widegap II–VI compounds for optoelectronic applications, Spinger-Science + Business Media, B.V., 1992.